

Electro-optic Ceramics and their Display Applications

Kenji Uchino

International Center for Actuators and Transducers, Materials Research Laboratory, The Pennsylvania State University, University Park, PA 16802, USA

(Received 3 October 1994; accepted 7 November 1994)

Abstract: Relaxor ferroelectrics are remarked in non-linear optic applications because an extraordinarily large apparent 'electro-optic Kerr effect' can be observed, even in the so-called paraelectric state. This paper describes the fundamental electro-optic properties of perovskite-type polycrystalline and single crystals, $\text{Pb}(\text{Zn}_{1/3}\text{Nb}_{2/3})\text{O}_3$, $(\text{Pb}, \text{La})(\text{Zr}, \text{Ti})\text{O}_3$ and $\text{Pb}(\text{Mg}_{1/3}\text{Nb}_{2/3})\text{O}_3\text{--PbTiO}_3$, firstly. Then, a new type of two-dimensional light valve array for an image projector is introduced. A light shutter array with 10×10 pixels was fabricated by a sophisticated tape casting technique. Plate-through and separate electrodes are stacked alternately so as to make vertical addressing by an external electrode connecting separate electrodes and horizontal addressing by a plate-through electrode. The applicative feasibility to a high definition image projector was verified.

1 INTRODUCTION

The electro-optic effect, which is the refractive indices change with an external applied electric field, will provide very promising useful devices such as light valves, deflectors, displays, etc., in the next optical communication age, in conjunction with solid state laser chips and optical fibers. Compared with liquid crystal devices, the ceramic electro-optic components, in general, possess advantages in response speed (μsec), particularly in falling time, durability for strong light illumination and contrast ratio (10^2)/gray scale (16 scales). On the other hand, the present ceramic components require relatively high drive voltage (1 kV) and production cost (\$ 100). Therefore, the development of a simple mass-production process and designing of electrode configurations with a narrow gap, as well as the improvement of material properties, will be the key factors to the actual commercialization of the ceramic optical components.

Let us review the principle of a light shutter utilizing the second-order electro-optic effect (Kerr effect), initially. The birefringence Δn is induced in

a crystal when an electric field E is applied:

$$\Delta n = -(1/2)Rn^3 E^2 \quad (1)$$

where $R (= R_{11} - R_{12})$ is the quadratic electro-optic coefficient and n is the original refractive index of the crystal. When this sample is placed between crossed polarizers arranged at the 45° direction with respect to the E direction, and light is transmitted transversely to the E field (Fig. 1), the output light intensity is represented by

$$I = I_0 A \sin^2[(\pi R n^3 L / 2\lambda) E^2] \quad (2)$$

where I_0 is the incident light intensity, A an equipment constant, L the optical path length (i.e. the sample thickness), and λ is the wavelength of the light. The voltage required for the first intensity maximum is an essential device parameter and called the half-wavelength voltage.

This paper describes the fundamental electro-optic properties of relaxor ferroelectrics, firstly, searching the possibility of new electro-optic materials. Then, the experimental data are given in detail on the $\text{Pb}(\text{Mg}_{1/3}\text{Nb}_{2/3})\text{O}_3\text{--PbTiO}_3$ system. Finally, a new type of two-dimensional light valve array for an image projector is introduced, which

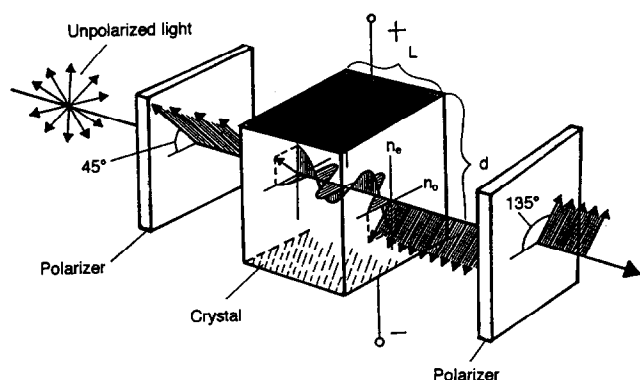


Fig. 1. Fundamental construction of an electro-optic light shutter.

can be mass-produced by a sophisticated tape casting technique. The drive voltage has been remarkably reduced, and FETs can be used directly for operation. This device will be a good candidate for the future high definition image projector.

2 CERAMIC ELECTRO-OPTIC MATERIALS

2.1 $\text{Pb}(\text{Zn}_{1/3}\text{Nb}_{2/3})\text{O}_3$

Relaxor ferroelectrics are remarked in non-linear optic applications because an extraordinarily large apparent 'electro-optic Kerr effect' can be observed, even in the so-called paraelectric state. Figure 2 shows the birefringence Δn vs electric field E relation of a $\text{Pb}(\text{Zn}_{1/3}\text{Nb}_{2/3})\text{O}_3$ single crystal in the paraelectric phase.¹ The single crystal sample was made by a flux method using excess PbO. The parabolic curve in the low field region tends to approach a straight line in the high field region.

A possible phenomenological analysis of this peculiar phenomenon is based on the model that

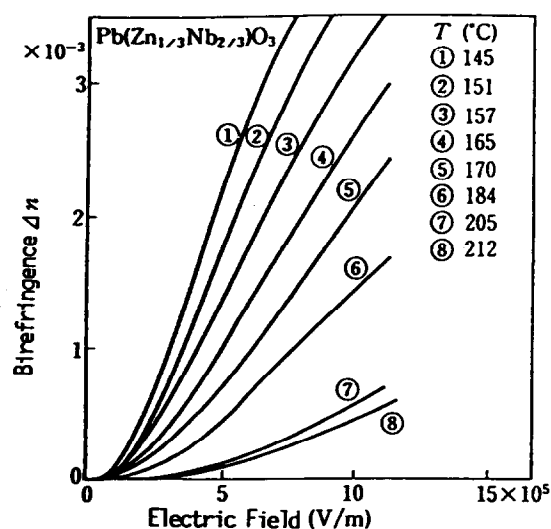


Fig. 2. Birefringence vs field in the paraelectric $\text{Pb}(\text{Zn}_{1/3}\text{Nb}_{2/3})\text{O}_3$.

the crystal is composed of the ferroelectric and paraelectric phases mixed together.¹ Suppose that the volume fraction of the paraelectric phase $x(T)$ is given by the accumulated Gaussian distribution with respect to temperature, the birefringence Δn is estimated by the summation of linear and quadratic electro-optic effects:²

$$\Delta n = [1 - x(T)] n^3(r_{33} - r_{13}) E/2 + x(T) n^3 R_{44} E^2/2 \quad (3)$$

where n is the refractive index, and r and R represent electro-optic Pockels and Kerr coefficients, respectively. Even if the experimental data can be explained phenomenologically, the actual situation may not be so simple as this model: $x(T)$ should also be a function of electric field E .

Another more realistic explanation is found in a microscopic domain reversal mechanism. $\text{Pb}(\text{Zn}_{1/3}\text{Nb}_{2/3})\text{O}_3$ exhibits very small spindle-like domains ($5 \mu\text{m}$) with ambiguous boundaries arranged perpendicularly to the external electric field. When a field above 0.5 kV/mm is applied, the ambiguous curve domain walls move simultaneously in a certain size region, so that each micro-domain should change synchronously like co-operative phenomena (see Fig. 3).³ It is noteworthy that the stripe period of the dark and bright domains (corresponding to up and down polarizations) will not be changed by the domain reversal, and that each domain area changes under an AC external field with zero net polarization at zero field. The relaxor crystal can be electrically-poled easily when an electric field is

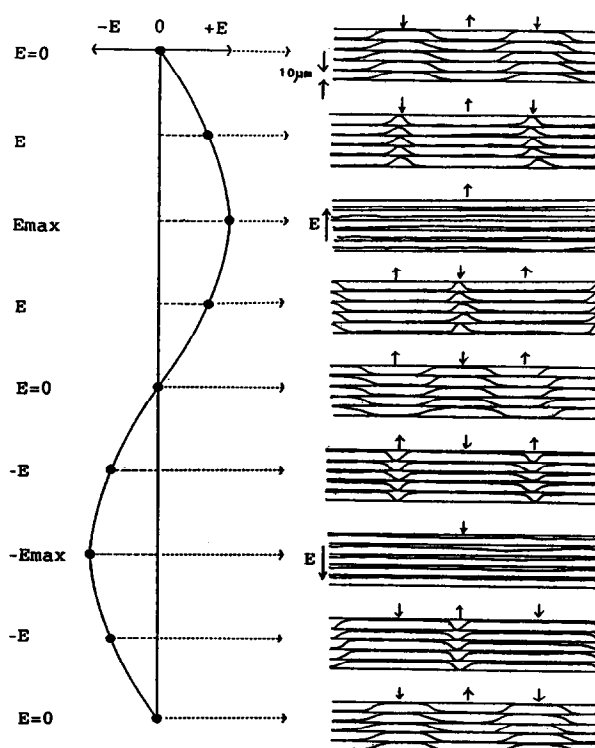


Fig. 3. Domain reversal mechanism in $\text{Pb}(\text{Zn}_{1/3}\text{Nb}_{2/3})\text{O}_3$.

applied around the transition temperature, and depoled completely without any remanent polarization. This can explain large 'apparent' secondary non-linear effects in physical properties such as electrostrictive and electro-optic Kerr phenomena, without exhibiting any hysteresis.

2.2 (Pb,La)(Zr,Ti)O₃

Famous transparent ceramics PLZT, i.e. (Pb_{1-x}La_x)(Zr_yTi_{1-x/4-y})O₃, are also an example of relaxor ferroelectrics, which exhibit large electro-optic effect ($R = 9.1 \times 10^{-16} \text{ m}^2\text{V}^{-2}$) near the composition 9/65/35 and are applicable to practical light shutters, displays, etc.

However, care must be taken for grain size control. Figure 4 shows the grain size dependence of the electro-optic coefficients, R and g (defined as $\Delta n = -(1/2)g n^3 P^2$), in PLZT 9/65/35.⁴ The samples were prepared by hot-press sintering starting from coprecipitated PLZT powders. The electro-optic response is drastically decreased below 2 μm , which corresponds approximately to the critical grain size below which the sample exhibits paraelectric properties.⁵ Therefore, relatively large grain size is necessary to reveal the reasonable electro-optic effect.

On the other hand, a serious problem arises in fracture toughness or durability for particularly large grain size samples, probably due to the deficient (B-site vacancy) crystal structure. A normally sintered transparent PLZT ceramic with an average grain size more than 6 μm has fracture toughness of $K_{IC} = 0.9 \text{ MNm}^{-3/2}$,⁵ which corresponds roughly to 10^8 cycles durability under repeating operation. This means only 2 months durability when the PLZT is used for an image display (TV) driven at 30Hz.

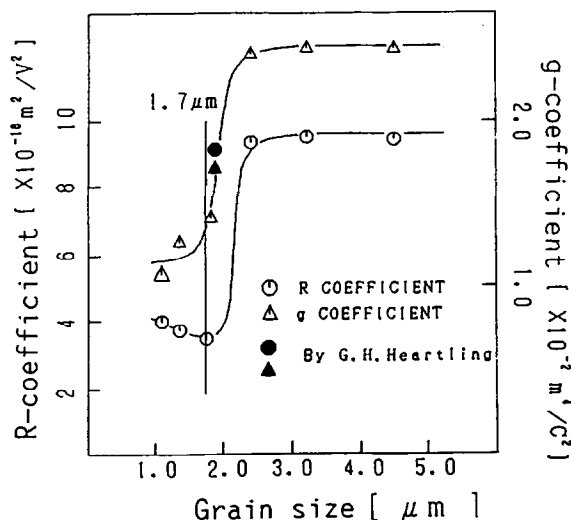


Fig. 4. Grain size dependence on the electro-optic coefficients, R and g , in PLZT 9/65/35.

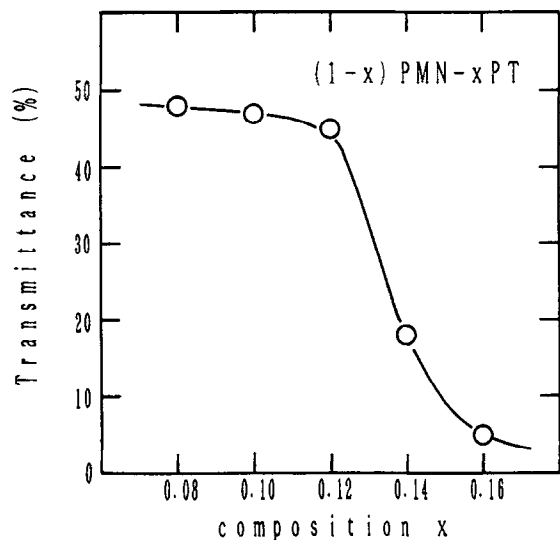


Fig. 5. Transmittance of a 0.5 mm thick sample for $\lambda = 633 \text{ nm}$ in $(1-x)\text{Pb}(\text{Mg}_{1/3}\text{Nb}_{2/3})\text{O}_3-x\text{PbTiO}_3$.

2.3 Pb(Mg_{1/3}Nb_{2/3})O₃-PbTiO₃

Discovery of a new ceramic electro-optic material with higher fracture toughness, as well as larger electro-optic coefficients, will be an urgent necessity for image display applications. The following conditions should be satisfied for the ceramic: (1) ceramic transparency requires almost zero birefringence in the original state (i.e. a pseudo-cubic structure) to suppress light scattering, (2) large fracture toughness may be obtained in a sufficiently packed structure, (3) large electro-optic effect is realized in relaxor ferroelectrics.

The $\text{Pb}(\text{Mg}_{1/3}\text{Nb}_{2/3})\text{O}_3\text{-PbTiO}_3$ system, which is known as a superior electrostrictive (secondary effect) material with very high fracture toughness ($K_{IC} = 1.7 \text{ MNm}^{-3/2}$), may be a good candidate to investigate from an electro-optic viewpoint. Samples

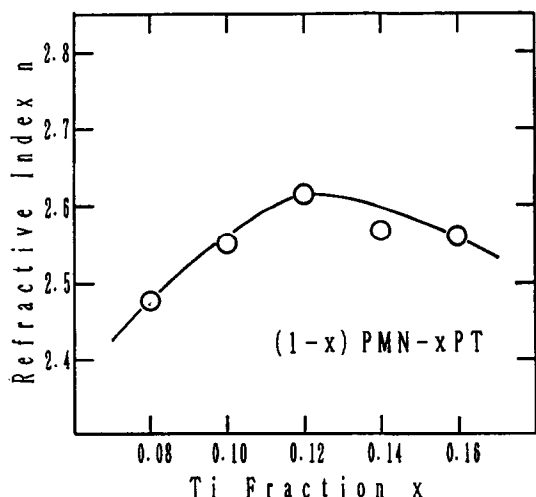


Fig. 6. Refractive index change in $(1-x)\text{Pb}(\text{Mg}_{1/3}\text{Nb}_{2/3})\text{O}_3-x\text{PbTiO}_3$.

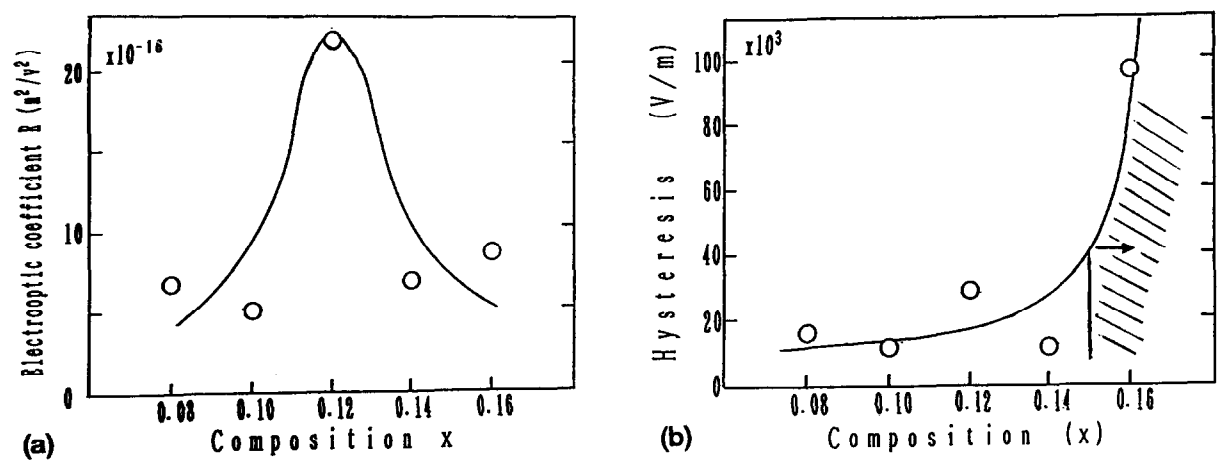


Fig. 7. Changes in (a) the electro-optic coefficient R and (b) the corresponding hysteresis in $(1-x)\text{Pb}(\text{Mg}_{1/3}\text{Nb}_{2/3})\text{O}_3-x\text{PbTiO}_3$.

of the $(1-x)\text{Pb}(\text{Mg}_{1/3}\text{Nb}_{2/3})\text{O}_3-x\text{PbTiO}_3$ system were prepared by hot-press sintering starting from the oxide mixtures. Note that the Curie temperature increases gradually with the PbTiO_3 content, passing room temperature around $x = 0.12$, and the crystal structure is pseudo-cubic in the region below $x = 0.4$. Figure 5 shows the composition x dependence of light transmittance ($\lambda = 633 \text{ nm}$) of a 0.5 mm thick sample in the $(1-x)\text{Pb}(\text{Mg}_{1/3}\text{Nb}_{2/3})\text{O}_3-x\text{PbTiO}_3$ system. The transmittance is reduced drastically above $x = 0.14$, probably due to the scattering caused by the spontaneous birefringence. The best transmittance (49%) is still smaller than 62% in the conventional PLZT; this suggests that more sophisticated powder preparation techniques will be required for the PMN-PT. The refractive index n ($\lambda = 633 \text{ nm}$) change with x is plotted in Fig. 6, which shows a small maximum around $x = 0.12$. The values are slightly larger than $n = 2.49$ in PLZT 10/65/35. The most intriguing data can be found in electro-optic measurements. Figures 7(a) and 7(b) show the electro-optic R coefficient and its corresponding hysteresis for $\lambda = 633 \text{ nm}$, respectively, plotted as a function of composition x . The maximum electro-optic R coefficient of $22 \times 10^{-16} \text{ m}^2/\text{V}^2$ for

$x = 0.12$ is more than twice as large as $9.1 \times 10^{-16} \text{ m}^2/\text{V}^2$ in the famous PLZT 9/65/35. The hysteresis, defined as an equivalent bias electric field to fit the experimental Δn curve by the quadratic relation of E , increases drastically above $x = 0.16$, the samples in which region can not be used practically.

In conclusion, $0.88 \text{ Pb}(\text{Mg}_{1/3}\text{Nb}_{2/3})\text{O}_3-0.12 \text{ PbTiO}_3$ will be the better electro-optic ceramic with high mechanical toughness, if better light transmission is obtained by improving the preparation technology.

3 TWO-DIMENSIONAL DISPLAYS

This section deals with a concept of a projection type TV utilizing two-dimensional PLZT displays. The development of a simple mass-production

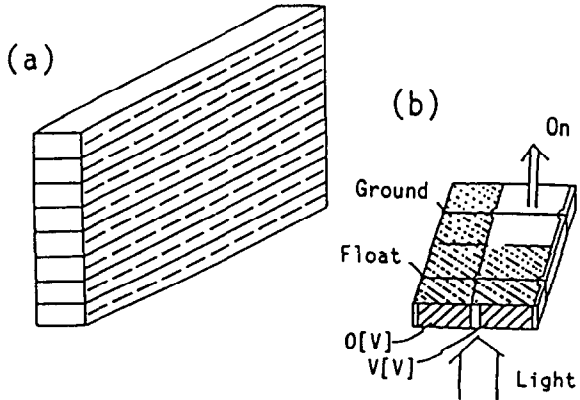


Fig. 8. Newly developed design of a two-dimensional display.

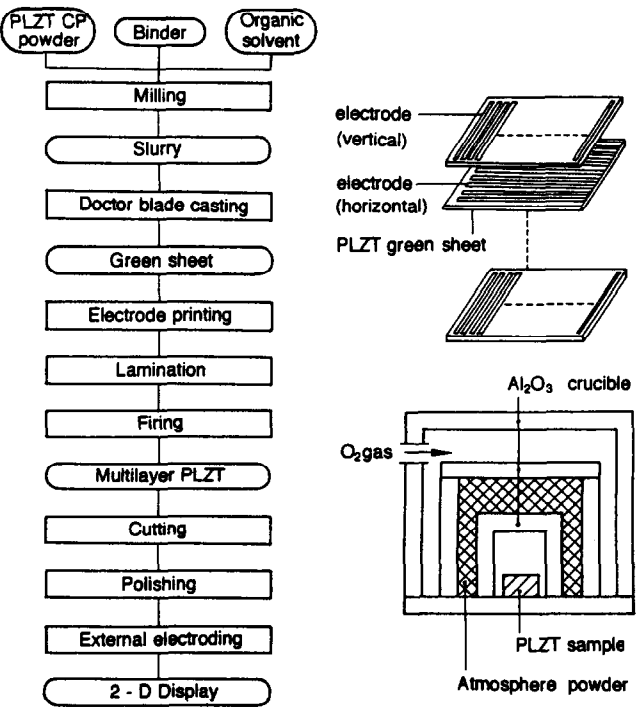


Fig. 9. Fabrication process of the new 2-D display.

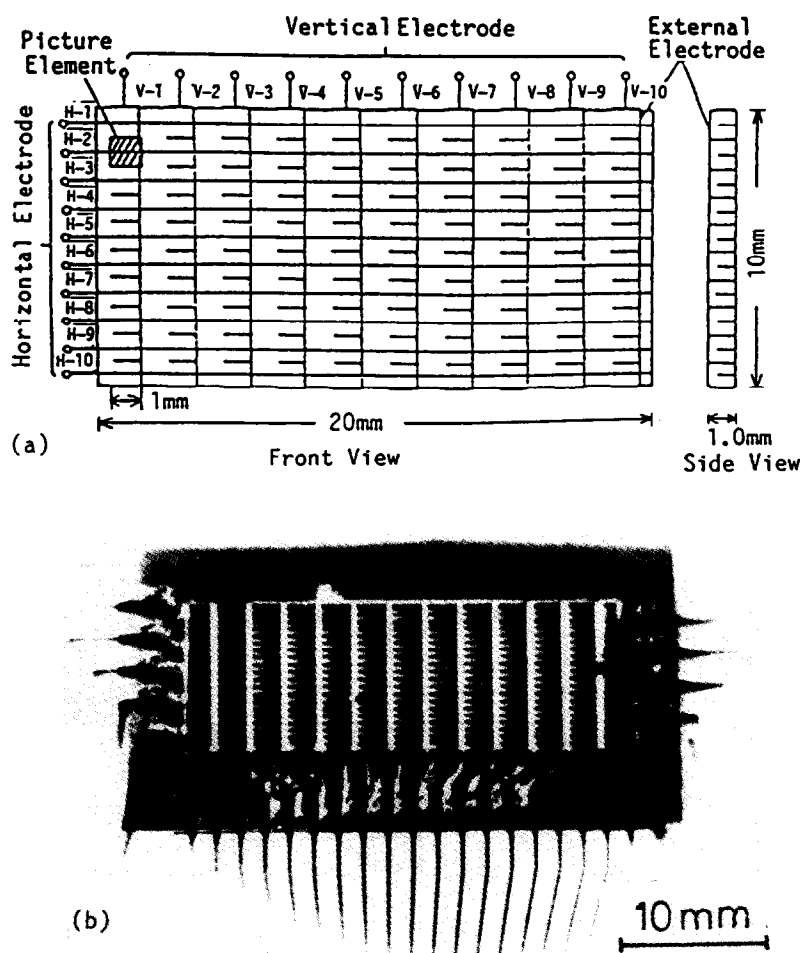


Fig. 10 (a) Schematic electrode configuration of a (10×10) matrix PLZT light valve. (b) Top view photograph of a PLZT light valve with external electrodes.

process and the designing of electrode configurations with a narrow gap are the key factors for the PLZT displays. A newly developed design, as shown in Fig. 8, presents a very bright image with a slight crosstalk-related problem and is easy to produce.

3.1 Fabrication process of the 2-D display

The fabrication process of the two-dimensional PLZT light valve array is outlined in Fig. 9.⁶ Coprecipitated PLZT 9/65/35 powders were mixed with organic solvent and binder and formed into a green sheet. Platinum internal electrodes were printed on the green sheets. The electroded sheets were then laminated alternately in 90° different orientations under a pressure of 3000 psi, so as to make plate-through and separate electrodes. The laminated body was sintered in an oxygen-controlled atmosphere, and the bulk was cut and polished. Finally the external connecting electrodes were applied to make vertical and horizontal addressing.

Figure 10(a) shows the electrode configuration of a (10×10) matrix light valve. The shaded portion of the device in the figure represents one

image unit (pixel). The vertical separate internal electrodes were connected by external electrodes printed on the surface of the device. The horizontal plate-through electrodes were embedded $100 \mu\text{m}$ deeper from the optical surface to avoid shorting with the vertical electrode connectors. Figure 10(b) shows a picture of the newly fabricated display. Note that the layer thickness is about 0.35 mm.

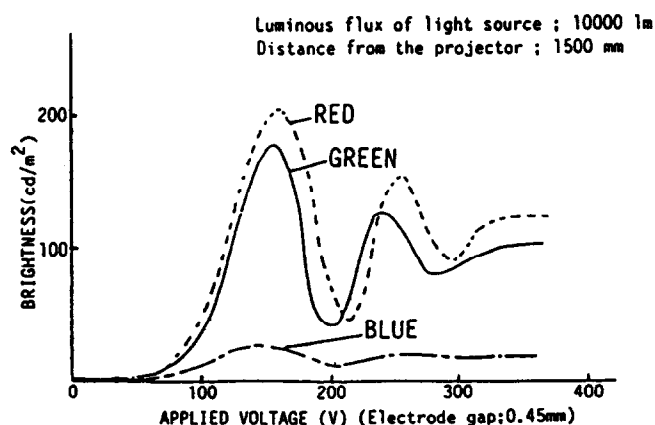


Fig. 11. Brightness on the screen vs applied voltage for red, green or blue light. Note that the half wavelength voltage differs for these three lights.

3.2 Characteristics of the light valve array

The optical transmittance of the PLZT device fabricated by the tape casting technique was 62% at $\lambda = 633$ nm, which is in good comparison with 63% for the ideal sample prepared by hot-pressing. The brightness for red, green and blue light was measured as a function of applied voltage (Fig.11), where the electrode gap was 0.45 mm.⁶ The contrast ratio, defined by a ratio of brightness on the screen under the application of half-wave-length voltage over brightness under zero volt ($220 \text{ cd/m}^2/2.8 \text{ cd/m}^2$), was about 80, rather superior to the values for the conventional cathode ray

tubes or liquid crystal displays. The response time associated with a single pixel of the display was less than $10 \mu\text{sec}$ for both rising and falling processes, which is rapid enough to drive this shutter array at a raster frequency of the conventional CRTs.

3.3 Construction of the image projector

The driving circuit of the display is represented schematically in Fig. 12(a). When the terminals of the device are addressed as shown in Fig. 12(b), the image appearing in Fig. 12(c) (alphabet 'F') is generated on the screen.⁶

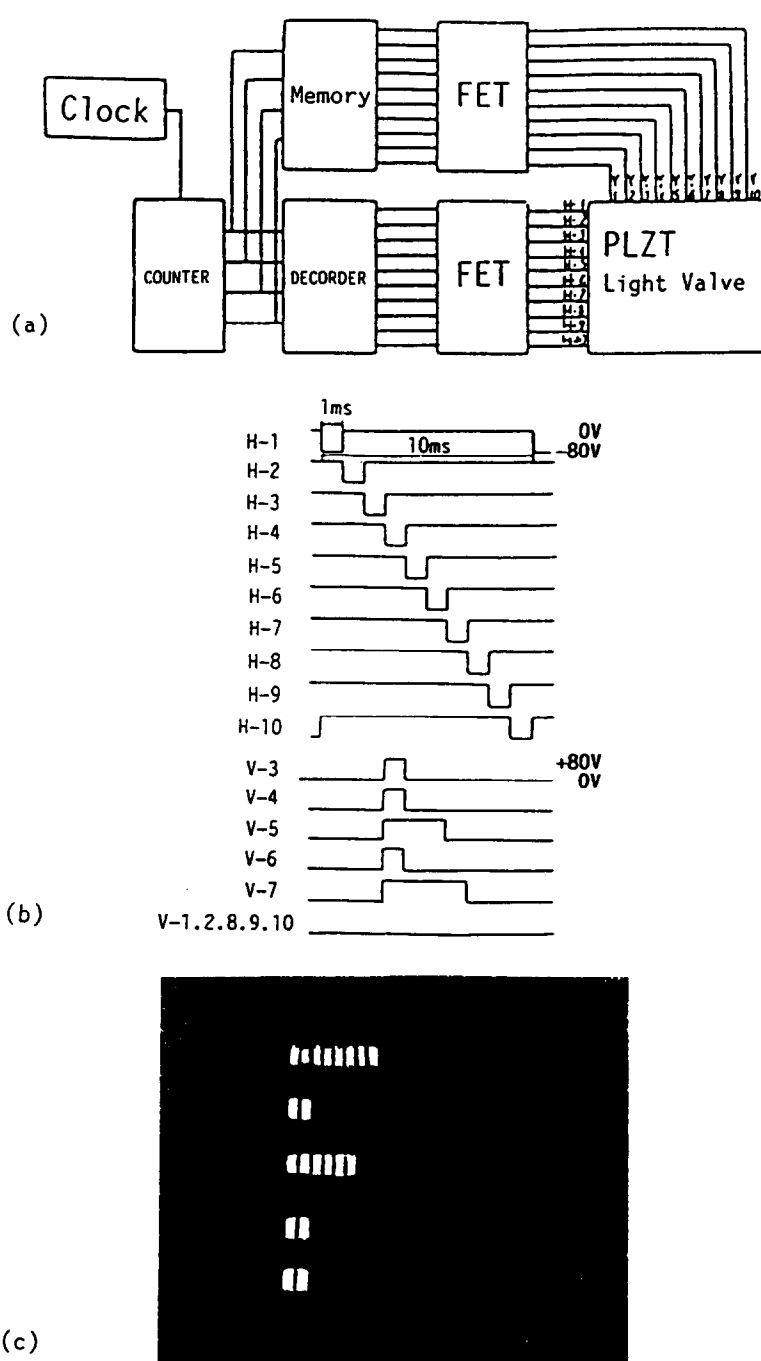


Fig. 12. (a) Driving circuit of the 2-D display. (b) Example wave forms of the driving signal. (c) An example image 'F' on the screen illuminated from the PLZT projector.

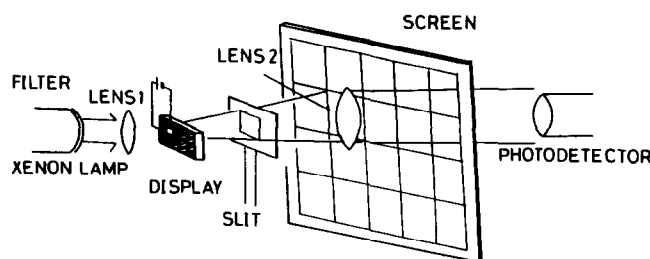


Fig. 13. Crosstalk test system. The light through a slit focused on the screen is measured.

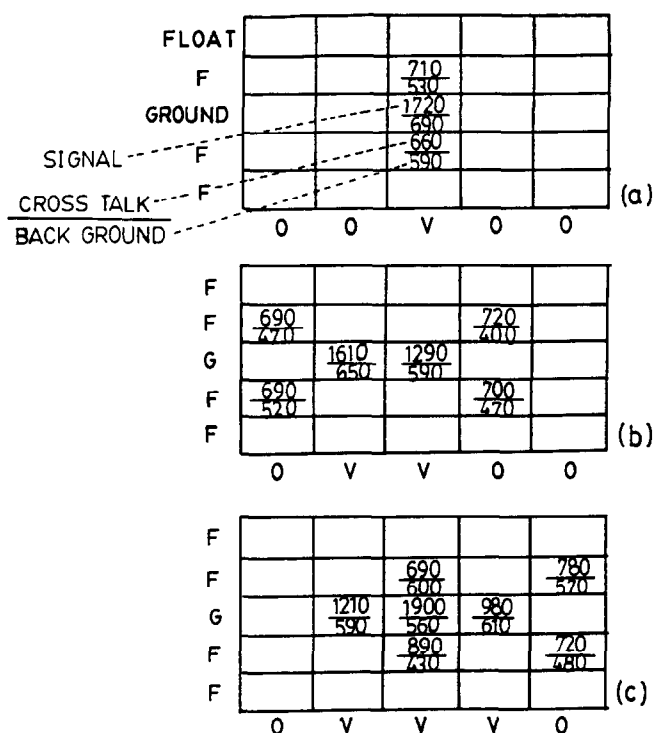


Fig. 14. Crosstalk patterns for different signal addressing: (a) Vertical type, (b) oblique type and (c) complex type.

Crosstalk phenomenon was checked on the 2-D display using a setup as illustrated in Fig. 13 with monochromatic light. The test was made with keeping one vertical terminal on (Ground) and applying high voltage on multiple horizontal terminals. There are three different crosstalk patterns: vertical, horizontal and oblique types. The results are shown in Fig. 14(a)–(c) for the different input number of horizontal terminals, where the top and bottom of a pair of figures indicate the

light intensity in μW unit on the screen in ON state and OFF state, respectively. The leakage light intensity associated with the vertical or horizontal crosstalk is 20–30% or 10–20% of the main peak intensity, which does not affect the image contrast significantly. On the contrary, the oblique type crosstalk causes not negligible leakage up to 50% depending on the applied voltage and the number of horizontal addressing input signal (combination type crosstalk). Modification of the internal electrode configurations will be necessary to avoid the crosstalk problem completely.

4 CONCLUSIONS

1. Relaxor ferroelectrics are widely applicable to electro-optic light valves/displays, etc. Superior characteristics of these materials are mainly attributed to the easy poling of the ferroelectric micro-domains.

2. A new electro-optic ceramic, $0.88\text{Pb}(\text{Mg}_{1/3}\text{Nb}_{2/3})\text{O}_3-0.12\text{PbTiO}_3$, with high mechanical toughness may provide a breakthrough for long-term display applications.

3. A new type of PLZT two-dimensional light valve fabricated by a tape casting technique has been developed, and a prototype image projector was investigated. It is easy to mass-produce, leading to a low manufacturing cost. This light valve exhibits bright image with a negligible crosstalk-related problem. It can be driven in quick response (10 μsec) by a relatively low drive voltage (100 V/0.35 mm gap) in comparison with the conventional PLZT devices. The applicative feasibility to a high definition image projector was verified.

REFERENCES

1. KOJIMA, F., KUWATA, J. & NOMURA, S., *Proc. 1st Meeting on Ferroelectric Materials and Applications*, Kyoto, 1977, pp. 155–58.
2. KUWATA, J., UCHINO, K. & NOMURA, S., *Ferroelectrics*, **22** (1979) 863–67.
3. UJIE, R. & UCHINO, K., *Proc. IEEE Ultrasonic Symp.*, pp. 725–28. Hawaii, 1990.
4. TOKIWA, K. & UCHINO, K., *Ferroelectrics*, **94** (1989) 87–92.
5. UCHINO, K. & TAKASU, T., *Inspec.*, **10** (1986) 29–33.
6. UCHINO, K., TOKIWA, K., GINIEWICZ, J., MURAI, Y. & OHMURA, K., *Ceram. Trans.*, **14** (1990) 297–310.